LETTER OPEN ACCESS

Evaluation of Pulse-Shaped Waveform Modulation for Event Camera-Based OCC Systems

Jaime Aranda Cubillo[1] | Victor Guerra[2] | Cesar Azurdia-Meza[3] | Jose Rabadan[1] | Rafael Perez-Jimenez[1]

[1]Institute for Technological Development and Innovation in Communications (IDeTIC), Universidad de las Palmas de Gran Canaria, Las Palmas de Gran Canaria, Las Palmas, Spain | [2]Pi Lighting Sarl, Sion, Switzerland | [3]Department of Electrical Engineering, Universidad de Chile, Santiago, Chile

Correspondence: Jaime Aranda Cubillo (jaime.aranda102@alu.ulpgc.es)

ABSTRACT

This study introduces an event camera-based optical camera communication system utilising pulse-shaped waveform modulation leveraging the camera's high temporal resolution and sensitivity. The proposed scheme demonstrates reliable performance under controlled indoor conditions with a fixed transmitter–receiver distance, achieving bit error rate values below 3.13×10^{-3} at data rates of 100 bit/s with mid-range receiver bias sensitivity and mid-high transmitter illumination. Although the experiments tested only four symbols, the flexible design supports higher-order modulation, which has the potential for increased data rates and more efficient bandwidth utilisation.

Introduction

Neuromorphic cameras, inspired by the neurobiological structures and functions of biological retinas, operate on principles distinct from conventional frame-based cameras. Rather than capturing entire frames at fixed intervals, they asynchronously and independently detect brightness changes at each pixel, generating discrete spikes (events) when the change exceeds a predefined threshold. This unique data acquisition method provides several advantages, including high temporal resolution (on the order of µs compared to ms in standard cameras), a wide dynamic range (120 dB vs. 60 dB), and significantly lower power consumption (less than 100 mW compared to up to 10 W for conventional cameras) [1].

Event cameras have gained significant traction in the industry. Leading companies like Sony and Qualcomm are exploring the integration of event sensors into future smartphone chips [2]. These cameras are expected to be adopted in a wide range of appli-

cations, including surveillance systems, autonomous vehicles, unmanned aerial vehicles, and more.

In the context of optical camera communication (OCC), event cameras present several advantages. They reduce energy consumption by eliminating redundant data, offer immunity to motion blur for reliable performance in dynamic environments, and exhibit adaptability to extreme lighting conditions, making them exceptionally well-suited for such applications.

Event cameras have already been proposed as receivers for OCC systems. Wang et al. used on–off keying (OOK) modulation, with LED 'on' representing binary '1' and 'off' representing binary '0,' achieving up to 4 kbps indoors and lossless transmission over 100 m at 500 bps in sunlight [3]. Perez-Ramirez et al. applied pulse position modulation (PPM), where binary '0' is a pulse at the start and '1' at the midpoint, achieving a BER of 1×10^{-4} at 500 symbols/s indoors [4]. Additionally, in a previous work we proposed *n*-pulse modulation, encoding symbols with different
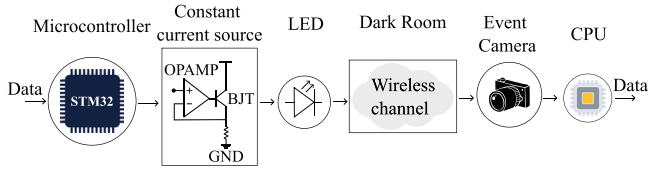
Fig. 1 │ Communication system pipeline, considering the transmitter, wireless channel and receiver.

Fig. 2 │ The figure on the left shows the transmitted symbol, the middle figure depicts the events generated during its reception, and the right figure presents the template or probability density function (PDF) estimated from events, using a Gaussian mixture model (GMM).

pulse counts, reaching a BER below 1.25×10^{-4} at 200 bit/s with four distinct symbols [5].

Existing modulation schemes based on traditional wireless techniques fail to fully exploit event cameras' unique features, limiting scalability to high-order modulation. The proposed system utilises a distinct pulse-shaped waveforms to represent symbols, effectively leveraging the high temporal resolution and sensitivity of event cameras. This design supports high-order modulation, allowing for increased data rates without the need for additional bandwidth.

System Description

The OCC system utilises an LED as the transmitter and an event camera as the receiver, as illustrated in the block diagram in Figure 1. Signal modulation is achieved through a pulse-shaping technique, where each symbol is represented by a distinct waveform. This approach leverages the event camera's sensitivity to brightness changes, resulting in unique event distributions at the receiver for each transmitted symbol, enabling the demodulator to detect symbols with high precision,

In this implementation, four distinct pulse-shaping waveforms-rectangular ('11'), rounded ('10'), triangular ('01'), and exponential pulse ('00')-are employed to encode 2 bits per symbol. These waveforms were selected for their simplicity in demonstrating the proposed scheme. Although the experiments were limited to four symbols, the flexible and scalable nature of this implementation allows the implementation of high-order modulation.

The transmitter consists of a 1 mm × 0.5 mm surface-mount device (SMD) LED (20 mA), powered by a constant current circuit to precisely control the brightness, given the event camera's high sensitivity to illumination changes. The STM32 microcontroller, equipped with a 12-bit digital-to-analogue converter (DAC), modulates the waveforms, allowing for precise control of the amplitude and symbol time of the light pulses. For the receiving end, we employ a commercial event camera, the DVXplorer, adjusting the image sensor's bias sensitivity to control parameters such as sensitivity, bandwidth, contrast threshold, and refractory period [5].

Demodulation is performed using a matching bank, where events generated from incoming unknown symbols are compared against four predefined templates, one for each pulse shaping waveform, constructed during a prior training stage. The template that best matches the incoming events-produced by the unknown transmitted symbol-is selected as the received symbol, enabling the recovery of the transmitted data.
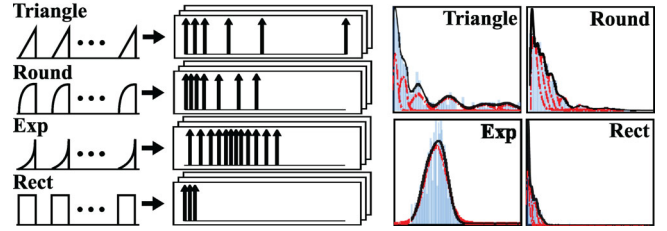
To build the templates, each symbol is transmitted multiple times during an initial training session, producing distinct event distributions at the receiver, as shown in Figure 2. The reception of different symbols results in variations in both, the temporal distribution and the number of events for each symbol. These variations make the symbols distinguishable within the receiver space. Based on the events collected at the receiver for each transmitted symbol, a probability density function (PDF) is estimated using Gaussian mixture models (GMM), with the expectation-maximisation (EM) algorithm employed to iteratively refine the model parameters [6]. The GMMs represent a weighted sum of multiple Gaussian distributions, each characterised by three parameters: the weight (π), the mean (μ), and the covariance (Σ). To ensure robust template estimation, each of the four symbols is transmitted separately, with fifteen replicas per symbol transmitted to ensure accurate PDF estimation.

The scheme was evaluated in terms of bit error rate (BER), defined as the ratio of incorrectly detected bits to the total transmitted bits. For the system evaluation, random words encoded in ASCII were transmitted, with each character represented by eight bits (seven for encoding and a leading '0'). These bits are then grouped into 2-bit symbols, which are mapped to their corresponding pulse-shaped waveforms. The scheme was tested under varying transmitter amplitudes, across four transmitter symbol rates, and three receiver bias sensitivity settings. The demodulation process can be mathematically described as follows. Let $\boldsymbol{e} = \{x_k, y_k, t_k\}_{k=1}^{K}$ represent the K positive events triggered by the reception of an unknown symbol, where each event occurs at pixel coordinates $(x_k, y_k)^T$ and time t_k. For each ith template, the likelihood function (L_i) is computed as,

$$L_i = \mathbb{P}(\boldsymbol{e}|\boldsymbol{\theta_i}) = \prod_{k=1}^{K} \mathbb{P}(e_k|\boldsymbol{\theta_i}) = \prod_{k=1}^{K} \sum_{m=1}^{M} \mathbb{P}(e_k|\mu_{i,m}, \Sigma_{i,m})\pi_{i,m} \quad (1)$$

with $\boldsymbol{\theta_i} = \{\mu_{i,m}, \Sigma_{i,m}, \pi_{i,m}\}_{m=1}^{M}$ the Gaussian distributions' parameters of the i-th template, $\mathbb{P}(e_k|\mu_{i,m}, \Sigma_{i,m}) = \mathcal{N}(e_k|\mu_{i,m}, \Sigma_{i,m})$ the mixture components, being $\mathcal{N}$ the normal distribution, and $\pi_{i,m}$ the mixture coefficients,

$$\sum_{m=1}^{M} \pi_{i,m} = 1, \ 0 \leq \pi_{i,m} \leq 1 \ \forall i. \quad (2)$$

The likelihood function quantifies the degree of correspondence between the set of received events $\boldsymbol{e}$, triggered by the reception of an unknown symbol, and each ith template. Specifically, it
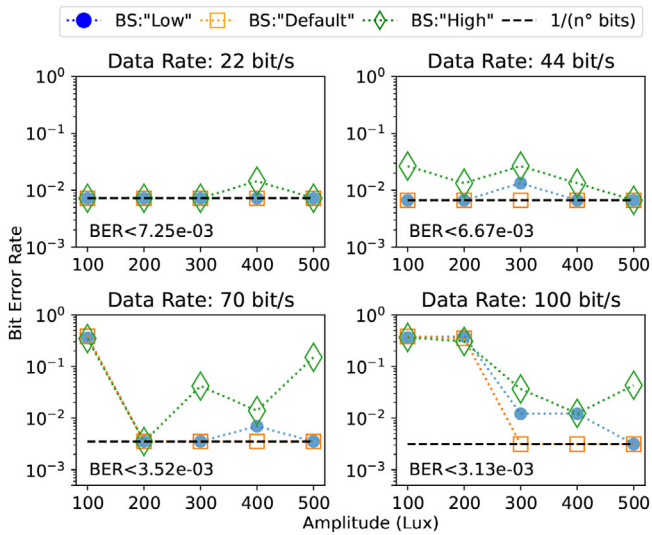
Fig. 3 | BER performance under varying transmitter and receiver parameters. The black dotted line indicates the minimum achievable BER, while the three coloured dotted lines represent results for different bias sensitivity (BS) levels.

provides a probabilistic measure of how closely the observed event distribution aligns with the previously obtained GMM template. The template with the highest likelihood score is selected as the detected symbol and subsequently mapped back to its corresponding 2-bit value, enabling the reconstruction of the transmitted data. This demodulation scheme is computationally efficient, based only on multiplications and summations for its computations.

Results

The experimental evaluation considering multiple transmitter and receiver parameters, including symbol rate, light intensity, and receiver bias sensitivity, to evaluate the system's performance in terms of bit error rate (BER) is presented in Figure 3. The experiments were carried out in a controlled dark room, maintaining a constant 2-m distance between the transmitter and receiver.

The results showed that as the transmitter symbol rate increases, the system performance degrades, as evidenced by the decreasing number of experiments achieving error-free communication. This degradation is attributed to the negative effect of the refractory period of the receiver's pixels. With increased transmitter symbol rates, pixel stimulation occurs more often, intensifying the effects of 'pixel dead time' and limiting the effective per-pixel sampling between events, reducing the system's ability to capture the signal dynamics accurately.

Considering the transmitter's light intensity, the system shows no significant differences in performance for lower data rates (11 and 22 bits/s), regardless of the light power levels. However, at higher symbol rates (35 and 50 bit/s), performance deteriorates significantly under low light intensity. This behaviour is explained by the reduced number of events triggered at the receiver when the light amplitude is insufficient. Coupled with the intensified

effects of the refractory period at higher symbol rates, the limited 'sampling' time per pixel hinders the reliable capture of signal dynamics, leading to degraded BER performance.

In addition, receiver bias sensitivity also plays a crucial role in system performance. The system performs best when the receiver is set to a mid-range sensitivity ('default'). Lower bias sensitivity values require a greater stimulus for the camera to generate events. Consequently, under lower light intensities, an insufficient number of events are triggered to capture the symbol dynamics accurately. On the other hand, higher bias sensitivity values enable the camera to detect events with smaller light intensity changes. However, these higher values exacerbate the effects of the refractory period, restricting the number of captured events and hindering accurate decision-making during the decoding stage.

Conclusion

The feasibility of optical camera communications using an event camera and a novel modulation scheme was evaluated. The experiments analysed BER for key parameters such as transmitter symbol rate, light intensity, and receiver bias sensitivity. Error-free links were achieved for most parameters, with BER values below 7.25×10^{-3} and 6.67×10^{-3} at 22 and 44 bit/s, respectively. At higher data rates, 70 and 100 bit/s, BER values below 3.52×10^{-3} and 3.13×10^{-3}, respectively, were achieved under medium-to-high light intensity conditions. The experiments confirmed that the event camera's bias sensitivity plays a crucial role in decoding accuracy, as both the refractory period and contrast threshold are directly influenced by it.

These results need to be validated under different conditions, such as larger distances between the transmitter and receiver and varying lighting environments. Additionally, it is necessary to develop a method for designing specific pulse-shaped wave-forms to improve symbol separation at the receiver space. This would enable the implementation of the system with a higher-order modulation scheme, achieving higher data rates without requiring additional bandwidth.

Author contributions

Jaime Aranda Cubillo: conceptualization, data curation, formal analysis, funding acquisition, investigation, methodology, resources, software, supervision, validation, visualization, writing – original draft, writing – review and editing. **Victor Guerra**: conceptualization, formal analysis, methodology, supervision, validation, writing – review and editing. **Cesar Azurdia – Meza**: supervision, validation, writing – review and editing. **Jose Rabadan**: conceptualization, validation, writing – review and editing. **Rafael Perez – Jimenez**: validation, writing – review and editing.

Conflicts of Interest

The authors declare no conflicts of interest.

Data Availability Statement

Data available on request due to privacy/ethical restrictions.

References

1. G. Gallego, T. Delbrück, G. Orchard, et al., "Event-Based Vision: A Survey," *IEEE Transactions on Pattern Analysis and Machine Intelligence* 44, no. 1 (2020): 154–180.

2. J. Chen, B. Y. Feng, H. Cai, et al., TimeRewind: Rewinding Time With Image-and-Events Video Diffusion, preprint, arXiv:2403.13800, March 20, 2024, https://doi.org/10.48550/arXiv.2403.13800.

3. Z. Wang, Y. Ng, J. Henderson, and R. Mahony, "Smart Visual Beacons With Asynchronous Optical Communications Using Event Cameras," in *2022 IEEE/RSJ International Conference on Intelligent Robots and Systems (IROS)* (IEEE, 2022), 3793–3799.

4. J. Perez-Ramirez, R. D. Roberts, A. P. Navik, N. Muralidharan, and H. Moustafa, "Optical Wireless Camera Communications Using Neuromorphic Vision Sensors," in *2019 IEEE International Conference on Communications Workshops (ICC Workshops)* (IEEE, 2019), 1–6.

5. J. Aranda, V. Guerra, J. Rabadan, and R. Perez-Jimenez, "Enhancing Computational Efficiency in Event-Based Optical Camera Communication Using N-Pulse Modulation," *Electronics* 13, no. 6 (2024): 1047.

6. N. Bouguila and W. Fan, *Mixture Models and Applications* (Springer, 2020).